THE ASTROPHYSICAL JOURNAL, 464:L47–L50, 1996 June 10

THE CLOSE ENVIRONMENT OF OJ 287: UNDERLYING NEBULOSITY AND A POSSIBLE OPTICAL JET?[1]

E. BENÍTEZ AND D. DULTZIN-HACYAN
Instituto de Astronomía–UNAM, Apdo. 70-264, 04510 México D.F., Mexico
J. HEIDT
Landessternwarte Königstuhl, D-69117 Heidelberg 1, Germany
AND
A. SILLANPÄÄ, K. NILSSON, T. PURSIMO, P. TEERIKORPI, AND L. O. TAKALO
Tuorla Observatory, Fin-21500 Piikkiö, Finland
Received 1996 January 24; accepted 1996 March 27

ABSTRACT

We present a deep *V*-band image of the BL Lac object OJ 287 and its close environment. Twenty-nine *V* images taken on 1994 January 18–21, when OJ 287 was at a low brightness level, were combined to obtain an image with a total integration time of 4.83 hr. The final image was processed using nonlinear restoration techniques (Lucy). The presence of a nebulosity surrounding OJ 287 can be distinctly seen for the first time in the deep image presented here. Comparing this image with radio maps obtained by Kollgaard et al. and Perlman & Stocke, we found that there is a coincidence between a faint optical elongation in the underlying nebulosity to the west of OJ 287 and the radio tail. Within 30″ of OJ 287, we can see several other interesting nearby features, such as three nearby companions at 3.″4, 6″, and 10″ projected distance, with colors of distant galaxies, and another elongation which seems to emerge from OJ 287 followed by an alignment of at least four features along a position angle of 220°. We discuss the possibility of this structure (or part of it) consisting of knots that form an optical jet. We also have *B*, *R*, *I*, and *K* images taken a posteriori at other sites, some obtained under subarcsecond seeing, which were used to determine the magnitudes and colors of some of the most relevant features surrounding OJ 287.

Subject headings: BL Lacertae objects: individual (OJ 287) — galaxies: active — galaxies: jets — galaxies: photometry

1. INTRODUCTION

BL Lac objects are the rarest, most enigmatic and violent variety of active nuclei. They are characterized by "featureless" optical spectra, variability in all wave bands and timescales, and high variable polarization. Blandford & Rees (1978) proposed that BL Lac objects are characterized by bulk relativistic motion in the emitting plasma very close to the line of sight.

Studies of the host galaxies and close surroundings of BL Lac objects address several important questions. First, they allow us to investigate whether the mechanism that triggers activity in these objects is related to interaction and/or merging processes, as seems to be the case for other active nuclei (e.g., Hutchings, Janson, & Neff 1989). Second, they are important for probing the "unified scheme" for active galactic nuclei (AGNs) by comparing the properties of the host galaxies of BL Lac objects with those of their apparent unbeamed parent population, the FR I radio galaxies (see recent review by Urry & Padovani 1995). Third, they provide a look at galaxy evolution over a wide redshift range. Fourth, it should be possible to find objects that may be affected by gravitational microlensing by searching for host galaxies which are offset with respect to the BL Lac core.

So far, most studies of BL Lac host galaxies were restricted to redshifts $z < 0.2$ (e.g., Abraham, McHardy, & Crawford 1991), and in very few cases up to $z = 0.6$ (Wurtz et al. 1993). Apart from one or two controversial cases (e.g., PKS 143+135; McHardy et al. 1994 and references therein), most of them were identified with luminous ellipticals. High-resolution imaging from the *Hubble Space Telescope* (*HST*) and from ground-based adaptive optics will provide new information on BL Lac environments at higher redshifts. There is, however, an open debate over the results of *HST* observations (see, e.g., Bahcall, Kirhakos, & Schneider 1995; McLeod & Rieke 1995). Thus it is particularly important to extend the studies of BL Lac host galaxies to higher redshifts using large telescopes and/or modern deconvolution and two-dimensional restoration techniques as we have done in this paper.

OJ 287 is one of the most active objects in the universe (e.g., Takalo 1994). Because of its exceptional activity and moderate redshift ($z = 0.306$), it is an especially interesting target for a study of its immediate vicinity.

In this work we present one of the results of the OJ 94 campaign. A very deep combined image with a total integration time of 4.83 hr was obtained from the monitoring on 1994 January, at the 2.1 m telescope of San Pedro Mártir Observatory, México, while OJ 287 was in a very faint state. This image disclosed an underlying nebulosity and several other interesting features. Further observations in the *B*, *R*, *I*, and *K* bands were made using the 2.5 m Nordic Optical Telescope at La Palma and the 2.2 m telescope at Calar Alto Observatory.

[1] Based on data collected at Observatorio Astronómico Nacional, San Pedro Mártir, Baja California, México; German-Spanish Astronomical Center, Calar Alto, operated by the Max-Planck-Institut für Astronomie jointly with the Spanish National Committee for Astronomy and the Nordic Optical Telescope at La Palma Observatory, Canary Islands, Spain.

2. OBSERVATIONS, DATA REDUCTION, AND PROCESSING

2.1. *Images*

2.1.1. *San Pedro Mártir Observations*

Twenty-nine images, out of more than 160, were selected to produce a deep, high signal-to-noise ratio image of OJ 287. The images, taken on 1994 January 14–21, when OJ 287 was in a very faint state ($V \sim 16$), were obtained with a 1024×1024 CCD coupled to the 2.1 m telescope. The plate scale was $0''.26$ pixel^{-1}. For details see Benítez, Dultzin-Hacyan, & Argaíz (1994). Only those frames taken under the best photometric and seeing conditions were used to construct a co-added image. Each image was reduced using IRAF standard techniques. The IRAF/IMSHIFT routine was used to make all frames coincide, and then IRAF/COMBINE to add the frames of each night in order to produce a final V frame. The signal-to-noise ratio of the co-added image was 6.5 times higher than the one measured for each single frame. The total integration time was 4.83 hr, and the limiting magnitude was $V \sim 25$.

The final frame was processed using the Richardson-Lucy algorithm (Lucy 1992). This program iterates the image until convergence is achieved. This occurs when the image reaches the resolution of the point-spread function (PSF) used in the algorithm for the deconvolution. The best star in the combined frame was used to define the PSF, which in this case has a resolution of $\sim 1''.7$. We achieved convergence after only one step. Unfortunately, the algorithm available to us produced Gibbs oscillations or "ringing" around OJ 287. This effect is produced when the "star" (in this case OJ 287) is superposed on an extended background source (an indirect confirmation of the fact that we do indeed have an extended underlying structure); for more details see Lucy (1994). The restored image is shown in Figures 1*a* and 1*b* (Plate L8), with an overlap of scaled radio contour maps from Kollgaard et al. (1992) and Perlman & Stocke (1994), respectively. Notice the coincidence of the radio tail to the west with a faint optical elongation in the same direction. Other coincidences are suggested by low-level radio contours in Figure 1*a*, although this last radio map is a factor of 5 times less sensitive than the one in Figure 1*b*.

2.1.2. *Nordic Optical Telescope Observations*

B, *R*, and *I* images of OJ 287 and its surroundings were obtained with the Nordic Optical Telescope (NOT) at La Palma, Canary Islands. Five *R*-band images were taken on the photometric nights of 1994 May 17–18, with the IAC CCD attached to the NOT, with a scale of $0''.14$ pixel^{-1}. These frames were combined to obtain a subarcsecond *R*-band image with FWHM $\sim 0''.6$ and a total integration time of 1000 s. In this image (not shown here; see Benítez et al. 1996), we can clearly resolve an innermost knot in the chain along a position angle of 220°. *B* and *I* images were acquired with the Brorfelde CCD attached also to the NOT, with a scale of $0''.176$ pixel^{-1}. The *I*-band images are from 1994 December 2, and the final combined image has an integration time of 600 s and a FWHM $\sim 0''.7$. Finally, on the same night a 600 s *B* image was obtained with a FWHM $\sim 0''.7$.

2.1.3. *Calar Alto Observations*

R-band observations were carried out on 1994 December 5 at the Calar Alto Observatory, using the 2.2 m telescope. The focal reducer CAFOS equipped with a Tektronix 1024×1024 CCD camera with a plate scale of $0''.49$ pixel^{-1} was used. The observing conditions were very good although not photometric. Three exposures with a total integration time of 70 minutes were taken, thus obtaining a deep *R* image. Between exposures the telescope had been shifted by $20''$. After standard reduction, the frames were made to coincide and were co-added. The final frame had a limiting magnitude of $R \sim 24.0$. The main features surrounding OJ 287 seen in the *V* image can also be distinguished in this deep *R* image. This image (not shown here) is, unfortunately, saturated in the locus of OJ 287. For this reason, restoration techniques were not applied to this image.

The *K*-band observations were carried out at the same telescope on 1995 February 20. The MAGIC camera was equipped with a NICMOS3 256×256 array (plate scale $0''.636$ pixel^{-1}). The observing conditions were photometric with good seeing ($\sim 1''.1$). OJ 287 was observed in a 3×3 mosaic, shifting the telescope by $15''$ between raster points. On each location three frames of 10 s were obtained, hence 27 observations for one cycle have been made. The cycle was repeated 27 times, providing a total integration time of 120 minutes. The image reduction and the combining procedure have been carried out in a manner similar to that described by McLeod & Rieke (1994). Full details are given in Heidt (1996). The final frame had a limiting magnitude of $K \sim 20.5$.

3. PHOTOMETRY

Nonlinear algorithms, such as the one used here, tend to degrade the photometric content of the data (Hook & Lucy 1994), so one cannot measure magnitudes from restored images. On the other hand, these algorithms are very successful at producing better contrast for morphological and identification purposes (see Cohen 1991; Linde & Spannare 1993). Hence, the combined restored image was used only to identify low-brightness features near OJ 287, as shown in Figure 1. Photometric measurements for objects around $30''$ of OJ 287 were carried out on the combined unrestored frame, using IRAF/DAOPHOT. This combined unrestored image was processed only to subtract the core of OJ 287 from the frame. To achieve this, a PSF was constructed from stars 4, 10, and 11 (Smith et al. 1985) in the frame and then subtracted from the locus of OJ 287. The reason for doing this is that we wanted to eliminate any possible contamination from the light of OJ 287 itself to its near companions. Finally, the image was convolved with a Gaussian kernel, and the result is shown in Figure 2. The negative contours around OJ 287 appear because the PSF is not constant over the entire image. Outside a radius of ~ 9–10 pixels the center of the stars is subtracted quite well, but inside this radius the results differ from star to star. The contours of Figure 2 are in arbitrary units, and the threshold as well as the dynamic range are different from those displayed in Figure 1. Thus, the difference in the appearance (apparent intensity) of some features is only due to a display artifice. A careful inspection shows, however, that the same features are present in both displays.

The calibrations of the *R* and *B* frames were done using stars C1 and C2 from Fiorucci & Tosti (1996), and for *I* and *V* we used stars 4, 10, and 11 from Smith et al. (1985). For the *K*-band observations, several standard stars from Elias et al. (1982) were observed during the night in order to set the zero point. In Table 1 we present *B*, *V*, *R*, *I*, and *K* magnitudes. The features in column (1) are those labeled in Figure 2. Columns

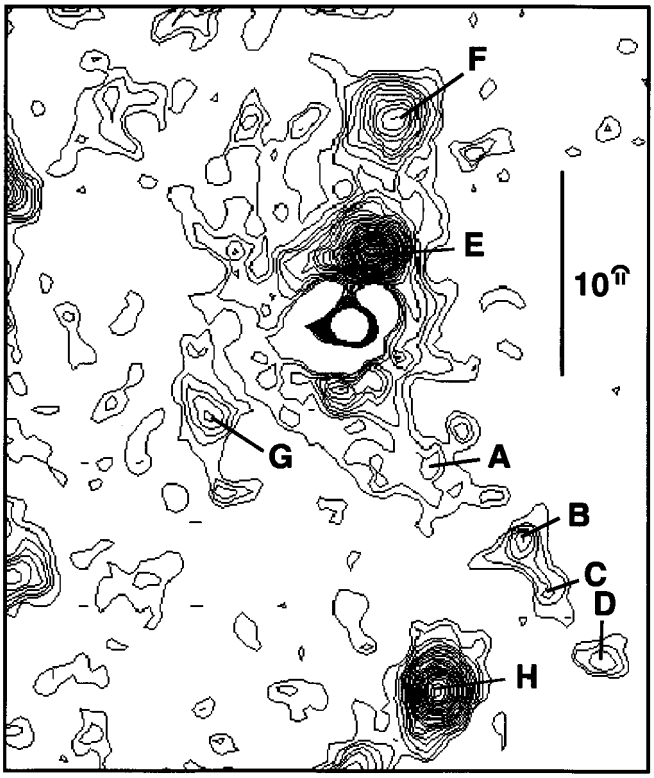

FIG. 2.—*V*-band combined image with OJ 287 subtracted using the PSF of stars in the frame. Labels correspond to the features in Table 1. North is at the top, and east is to the left.

(2)–(6) give magnitudes with errors, for each band. The apertures for *B* and *I* were 2.″11; for *V* and *K*, 2.″00; and for *R*, 1.″68. Exceptions are given in the footnotes to Table 1.

4. FINAL COMMENTS AND DISCUSSION

Early detections of a "fuzz" around OJ 287 were made by Kinman (1975). More recent claims for detection of the host galaxy are found in Hutchings & Neff (1990) and Wright, McHardy, & Abraham (1996). These detections are all based on one-dimensional analysis, i.e., profile extraction. In this Letter we apply two-dimensional techniques for the first time and thus eliminate the possibility of "contaminating" the profile with the presence of very near companions, all of which we can neatly resolve. We estimate a size for the host galaxy of 38 kpc (here and in what follows we use $H_0 = 50$, $g_0 = 0.5$), in very good agreement with the estimate by Hutchings & Neff (1990). These authors also give an estimate of the absolute *R*-band magnitude of the host galaxy of −22.6.

A striking result is the coincidence of an optical filament and a radio tail to the west reported by Kollgaard et al. (1992) and Perlman & Stocke (1994). This filament is neatly seen in the raw co-added image, and thus it cannot be produced in any artificial way by the restoration process. A similar structure has recently been found in the QSO 1302−102 by Hutchings et al. (1994). Unfortunately, we cannot comment on the physical association of the optical and radio emission at present. However, if the emission of these features turns out to be indeed related, and comes from a jet, this would be the first such case found for a BL Lac–type object. Deeper optical images in different colors and a better radio map of that region are certainly needed.

A conspicuous elongated feature seems to emerge from OJ 287 at P.A. 220°, with a projected length of 22″ (measured from the center to feature D). If this feature is indeed related to OJ 287, its projected length is ∼122 kpc. One possible interpretation of this elongation is that it is an optical jet emerging from OJ 287; this would be the longest optical jet ever observed in a BL Lac object. The other interpretation is a chance alignment of galaxies and/or stars. The probability of a chance alignment or chain of physically related galaxies is extremely low, although the galaxy chain in VV 172 (Arp 1966), if brought to the distance of OJ 287, would be of comparable size. Alternatively, this structure could result from a chance alignment of unrelated background galaxies and foreground stars. This last alternative is sustained by the fact that two out of eight features presented in Figure 1 and Table 1, have a stellar PSF (these are precisely features B and C). Moreover, their colors are in the range found for M and K stars, respectively (Johnson 1966). Comparison of the colors of the features along this elongation with those of the knots along the 3C 273 optical jet can be made using the flux densities reported in Röser & Meisenheimer (1991). We have all three colors only for our feature D, and these colors are similar to those of knot D in 3C 273. The $R-I$ colors of our features B and C, as well as the $B-R$ color of feature A, are all redder than those of any knot in the 3C 273 jet. However, this comparison has to be taken with caution, since the *K* corrections (which have not been applied in either case) are very different for each object—not to mention the fact that the observing apertures are also different. On the other hand, having two optical jets would be indeed extraordinary! Long-

TABLE 1

B, *V*, *R*, *I*, AND *K* PHOTOMETRY OF OJ 287 ENVIRONMENT

Feature (1)	$B \pm \sigma_B$ (2)	$V \pm \sigma_V$ (3)	$R \pm \sigma_R$ (4)	$I \pm \sigma_I$ (5)	$K \pm \sigma_K$ (6)
A.....	24.19 ± 0.19	24.15 ± 0.23	23.00 ± 0.24	...	...
B.....	...	23.62 ± 0.15	22.07 ± 0.12	20.82 ± 0.09	18.31 ± 0.09
C.....	...	24.02 ± 0.21	23.0 ± 0.22	21.83 ± 0.12	20.46 ± 0.38
D.....	24.22 ± 0.18	24.02 ± 0.22	23.45 ± 0.32	22.52 ± 0.20	19.76 ± 0.28
E.....	23.90 ± 0.14	21.74 ± 0.06	21.28 ± 0.09	20.43 ± 0.03	18.57 ± 0.19
F.....	22.44 ± 0.09	22.56 ± 0.07	21.89 ± 0.28	20.75 ± 0.19	20.15 ± 0.20
G.....	23.99 ± 0.16	23.97 ± 0.19	22.97 ± 0.24	...	...
H.....	23.04[a] ± 0.08	21.96 ± 0.06	21.33[b] ± 0.14	20.92[a] ± 0.10	18.49 ± 0.13

[a] Aperture is 2.″82.
[b] Aperture is 4.″48.

slit spectra of these elongations would help to elucidate their nature; this is a difficult but important future task.

We can clearly see the two objects to the north, labeled E and F in Figure 2, reported previously by Stickel, Fried, & Kühr (1993). In that paper, the nearest object, at 3″.4, can barely be distinguished from the isophote distortion. In our images it can be distinctly seen. The projected distance of this object to OJ 287 is only 19 kpc. We also see a distinct feature 6″ to the southeast (labeled "G" in Fig. 2), with similar colors. There is a hint of coincidences between features F and G and low-level radio contours (Fig. 1*a*).

With respect to all the other nearby nonstellar features, their colors are unusual, making it difficult to set constraints on their redshifts. Assuming that all the nonstellar features within 10″ radius around OJ 287 are galaxies at the same redshift, there would be four galaxies within a projected distance of ~60 kpc. Their absolute magnitudes are significantly fainter than that of an L^* galaxy (~2–3 mag in V assuming an L^* magnitude of $M_V = -21.0$; see, e.g., Efstathiou, Ellis, & Peterson 1988). Very nearby companion galaxies are found for other BL Lac objects also, as reported recently by Pesce, Falomo, & Treves (1995). This scenario supports the view that the BL Lac–type objects may be related to interactions of galaxies, as seems to be the case for many quasars (e.g., Hutchings et al. 1989) and Seyfert galaxies (e.g., Dahari 1984).

Sillanpää et al. (1988) proposed a model for the long-term variability behavior of OJ 287 based on a binary black hole in the center (see also Lehto & Valtonen 1996 and Sillanpää et al. 1996). A binary black hole may be produced by merger or interaction processes of galaxies harboring a black hole. Our findings suggest that we may indeed be seeing such a system in the vicinity of OJ 287. The characteristics of the larger size surroundings of OJ 287, as well as spectroscopy of the brightest features, will be discussed in detail in a subsequent paper (Heidt 1996).

This work was supported in part by DGAPA-UNAM through grant IN 107094, by the Finnish Academy of Sciences, and by the Deutsche Forschungsgemeinschaft through grant SFB 328. Part of the observations were taken within the OJ 94 project, which used the CCI 5% International Time on the Canary Islands telescopes for winter 1993/1994. The image reductions were done partly with the NOAO Image Reduction and Analysis Facility (IRAF). We acknowledge the suggestions of an anonymous referee, which helped to improve this Letter.

REFERENCES

Abraham, R. G., McHardy, I. M., & Crawford, C. S. 1991, MNRAS, 252, 482
Arp, H. 1966, ApJS, 123, 1
Bahcall, J. N., Kirhakos, S., & Schneider, D. P. 1995, ApJ, 450, 486
Benítez, E., Dultzin-Hacyan, D., & Argaíz, D. 1994, in Proc. Workshop on Intensive Monitoring of OJ 287, ed. M. R. Kidger & L. O. Takalo (Tuorla Obs. Rep. 174; Turku: Univ. Turku), 74
Benítez, E., Dultzin-Hacyan, D., Sillanpää, A., Nilsson, K., Pursimo, T., Teerikorpi, P., & Takalo, L. O. 1996, in Proc. Workshop on Two Years of Intensive Monitoring of OJ 287 and 3C 66A, ed. L. O. Takalo (Tuorla Obs. Rep. 176; Turku: Univ. Turku), 92
Blandford, R. D., & Rees, M. J. 1978, in Proc. Pittsburgh Conf. on BL Lac Objects, ed. A. N. Wolfe (Pittsburgh: Univ. Pittsburgh), 328
Cohen, J. G. 1991, AJ, 101, 734
Dahari, O. 1984, AJ, 89, 966
Efstathiou, G., Ellis, R. S., & Peterson, B. A. 1988, MNRAS, 232, 431
Elias, H. J., Frogel, J. A., Matthews, K., & Neugebauer, G. 1982, AJ, 87, 1029
Fiorucci, M., & Tosti, G. 1996, A&AS, 117, 1
Heidt, J. 1996, in Proc. Workshop on Two Years of Intensive Monitoring of OJ 287 and 3C 66A, ed. L. O. Takalo (Tuorla Obs. Rep. 176; Turku: Univ. Turku), 86
Hook, R. N., & Lucy, L. B. 1994, in Proc. Conf. on Restoration of *HST* Images and Spectra II, ed. R. J. Hanisch & R. L. White (Baltimore: STScI), 86
Hutchings, J. B., Janson, T., & Neff, S. G. 1989, ApJ, 342, 660
Hutchings, J. B., Morris, S. C., Gower, A. C., & Lister, M. L. 1994, PASP, 106, 642
Hutchings, J. B., & Neff, S. G. 1990, AJ, 99, 1715
Johnson, H. L. 1966, ARA&A, 4, 193
Kinman, T. D. 1975, in IAU Symp. 67, Variable Stars and Stellar Evolution, ed. V. E. Sherwood & L. Plant (Dordrecht: Reidel), 573
Kollgaard, R. I., Wardle, J. F. C., Roberts, D. H., & Gabuzda, D. C. 1992, AJ, 104, 1687
Lehto, H. J., & Valtonen, M. J. 1996, ApJ, 460, 207
Linde, P., & Spannare, S. 1993, in Proc. Fifth ESO Data Analysis Workshop, ed. P. Grosbøl & R. C. E. de Ruijsscher (Garching: ESO), 131
Lucy, L. B. 1992, in STScI Workshop Science with the *HST*, ed. P. Benvenuti & E. Shreier (Garching: ESO), 207
———. 1994, in Proc. Conf. on Restoration of *HST* Images and Spectra II, ed. R. J. Hanisch & R. L. White (Baltimore: STScI), 79
McHardy, I. M., Merrifield, M. R., Abraham, R. G., & Crawford, C. S. 1994, MNRAS, 268, 681
McLeod, K. K., & Rieke, G. H. 1994, ApJ, 420, 58
———. 1995, ApJ, 454, L77
Perlman, E. S., & Stocke, J. T. 1994, AJ, 108, 56
Pesce, J. E., Falomo, R., & Treves, A. 1995, AJ, 110, 1554
Röser, H.-J., & Meisenheimer, K. 1991, A&A, 252, 458
Sillanpää, A., Haarala, S., Valtonen, M., Sundelius, B., & Byrd, G. G. 1988, ApJ, 325, 628
Sillanpää, A., et al. 1996, A&A, 305, L17
Smith, P. S., Balonek, T. J., Heckert, P. A., Elson, R., & Schmidt, G. D. 1985, AJ, 90, 1184
Stickel, M., Fried, J. W., & Kühr, H. 1993, A&AS, 98, 393
Takalo, L. O. 1994, Vistas Astron., 38, 77
Urry, C. M., & Padovani, P. 1995, PASP, 107, 803
Wright, S. C., McHardy, I. M., & Abraham, R. G. 1996, in Proc. Workshop on Two Years of Intensive Monitoring of OJ 287 and 3C 66A, ed. L. O. Takalo (Tuorla Obs. Rep. 176; Turku: Univ. Turku), 98
Wurtz, R., Ellingson, E., Stocke, J. T., & Yee, H. K. C. 1993, AJ, 106, 869

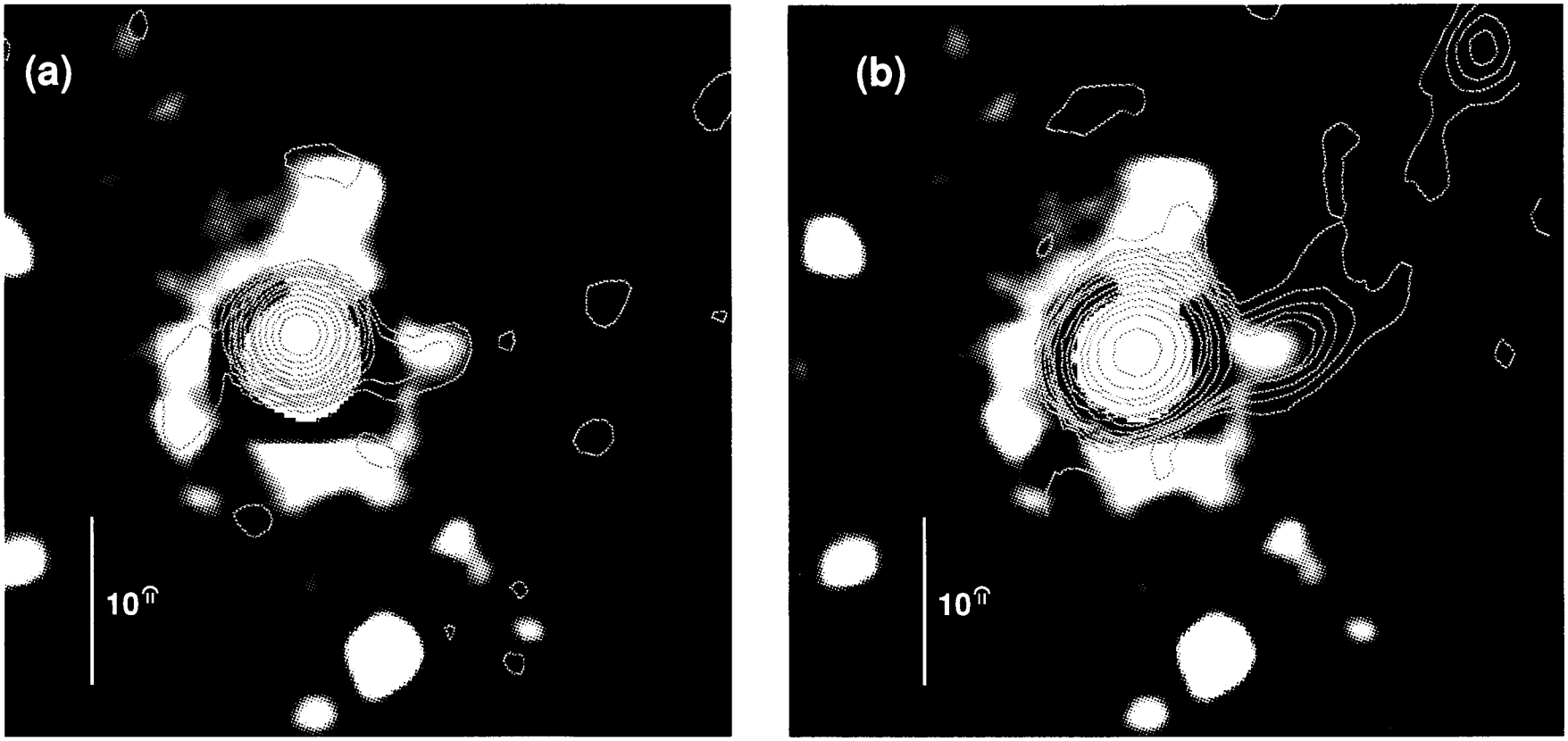

FIG. 1.—Combined V image with a total integration time of 4.83 hr. The Richardson-Lucy algorithm was applied to restore this image. (*a*) A scaled radio contour map obtained by Kollgaard et al. (1992) has been overlapped. (*b*) A scaled radio contour map obtained by Perlman & Stocke (1994) has been overlapped. North is at the top, and east is to the left.

BENÍTEZ et al. (see 464, L48)